

Directed Nanoparticle Binding onto Microphase-Separated Block Copolymer Thin Films

Wolfgang H. Binder,^{*,†} Christian Kluger,[†]
Christoph J. Straif,[‡] and Gernot Friedbacher^{*}

Institute of Applied Synthetic Chemistry/Division Macromolecular Chemistry, Vienna University of Technology, Getreidemarkt 9/163/MC, A-1060 Wien, Austria, and Institute of Chemical Technologies and Analytics, Vienna University of Technology, Getreidemarkt 9/164 IAC, A-1060 Wien, Austria

Received August 18, 2005

Revised Manuscript Received October 4, 2005

Introduction. The binding of nanoparticles (NPs) onto polymeric surfaces is an important step in generating ordered particle arrays.¹ Usually, self-assembly processes are required to direct nanocrystals with sizes from ~ 1 nm up to tens of nanometers onto functional surfaces. Critical for this binding and deposition process is (a) the control of the chemical nature of the surface onto which the NPs are bound, (b) the structure of the surface of the nanoparticles, in particular the chemical moieties bound, and (c) the tuning of the supramolecular interaction acting between the NP surface and the polymeric surface in terms of binding strength, binding multiplicity, and binding kinetics. In the past, several NP/surface systems relying on self-assembled monolayers (SAM's) have been reported. Supramolecular interactions (such as Reinhoudt's molecular printboards (relying on adamantane/cyclodextrine interactions),^{2,3} hydrogen-bonding systems (i.e., triazine/thymine binding system,⁴ Hamilton receptor/barbituric acid systems,⁵ and other conventional hydrogen bonds⁶), DNA-based systems,⁷ and purely electrostatically assembly⁸ have been used for this purpose. Besides other approaches (i.e., interfacial assembly, crystallization of opals),⁹ the supramolecular approach is still the most versatile in that it allows the spatially separated use of several interactions and thus the binding of several NPs on different parts of a surface. These supramolecular binding concepts have been transferred to the incorporation of NPs into polymeric matrices,¹⁰ although using widely nonspecific interactions, i.e., purely hydrophobic incorporation,¹¹ polymer/polymer interactions,¹² polymer/metal interactions, and single hydrogen bonds.¹³ Another approach starts with block copolymeric micelles in solution, into which nanoparticles have been incorporated and subsequently deposited onto surfaces, presenting the nanoparticles at a specific interface.¹⁴ Highly specific supramolecular interactions to direct nanoparticle binding on polymeric surfaces have—to the best of our knowledge—not been reported to date.

In the present paper we report on the binding of Au NPs onto microphase-separated polymeric films deposited on surfaces, where a strong (highly specific) hydrogen-bonding interaction has been positioned in one of the polymeric blocks of a block copolymer (BCP-1) (see

Figure 1). The relevant interaction relies on the Hamilton receptor/barbituric acid interaction, which comprises a binding strength of 10^4 – 10^6 M⁻¹, depending on whether the receptor is bound to polymers, oligomers, or surfaces. Thus, the Hamilton receptor has been incorporated 50-fold into one block of the BCP, and the barbituric acid has been fixed to the surface of Au nanoparticles. In contrast to previous investigations (where the incorporation of the NPs is accomplished directly in the bulk microphases of a BCP such as PVP-PS),^{12b} we have first prepared a microphase-separated film of a BCP and subsequently bound the NPs with the matching (barbituric acid) functionality. This approach yields a stable, highly specific NP attachment onto specific BCP phases on surfaces.

Experimental Section. a. Instrumentation. NMR spectra were obtained with a 200 MHz Bruker AC200 spectrometer and a 400 MHz Bruker Avance DRX 400 MHz in CDCl₃ and DMSO-*d*₆. GPC analysis was performed on a Viscotek VE 2001 system using Styragel linear columns in THF at 40 °C. Polystyrene standards were used for conventional external calibration using a Waters RI 2410 refractive index detector.

b. Materials. THF was dried by distillation from potassium and benzophenone, and CH₂Cl₂ was freshly distilled from CaH₂. All solvents used during the polymerization process as well as for postmodification reactions were dried and deaerated thoroughly. All reaction vessels were heated and flushed with argon before use. All chemicals were purchased from Sigma-Aldrich. *exo*-Oxabicyclo[2.2.1]hept-5-ene-2,3-dicarboximide,¹⁵ *exo*-N-(6-bromohexyl)-7-oxabicyclo[2.2.1]hept-5-ene-2,3-dicarboximide (5),¹⁶ and 5-hex-5-ynoylamino-N,N'-bis(6-octanoylamino)pyridin-2-yl)isophthalamide⁵ were prepared according to the literature. Preparation of the block copolymers BCP-1, BCP-2, and BCP-3 is given in the Supporting Information. *Au nanoparticles* (5 nm, bearing barbituric acid moieties) were prepared according to the literature.⁵ *Polymer films* were prepared on Wacker Siltronic silicon wafers by dip coating (3 mm/min) from a 0.5% solution in THF solution. Annealing of the polymeric films was carried out at 80 °C under vacuum for 48 h. *Nanoparticle binding:* nanoparticle solutions of 0.1–0.3% in toluene were sonicated for 5 min prior to use and directly used for the assembly experiments onto the polymer films. Assembling nanoparticles onto polymeric films was carried out at room temperature in toluene solutions for 16 h without stirring. The films were purified once with pure toluene and blow-dried with nitrogen gas. Then, AFM experiments were performed directly on these substrates. Monomer 4 was prepared as described in the Supporting Information.

c. AFM Measurement. For the AFM investigations a NanoScope III multimode SPM from Digital Instruments, Veeco Metrology Group, Santa Barbara, CA, has been used. Measurements were performed in tapping mode under ambient air using single-crystal silicon cantilevers (Arrow NC cantilevers, NanoWorld, Switzerland, spring constant 42 N/m, resonance frequency ~ 285 kHz). Scanning was accomplished with an E-scanner (maximum scan range $10\ \mu\text{m} \times 10\ \mu\text{m}$) operated at a scanning rate of 2 Hz and an image resolution of 512×512 pixels. Data evaluation was performed with

[†] Institute of Applied Synthetic Chemistry/Division Macromolecular Chemistry.

^{*} Institute of Chemical Technologies and Analytics.

^{*} Corresponding author. E-mail: wbinder@mail.zserv.tuwien.ac.at.

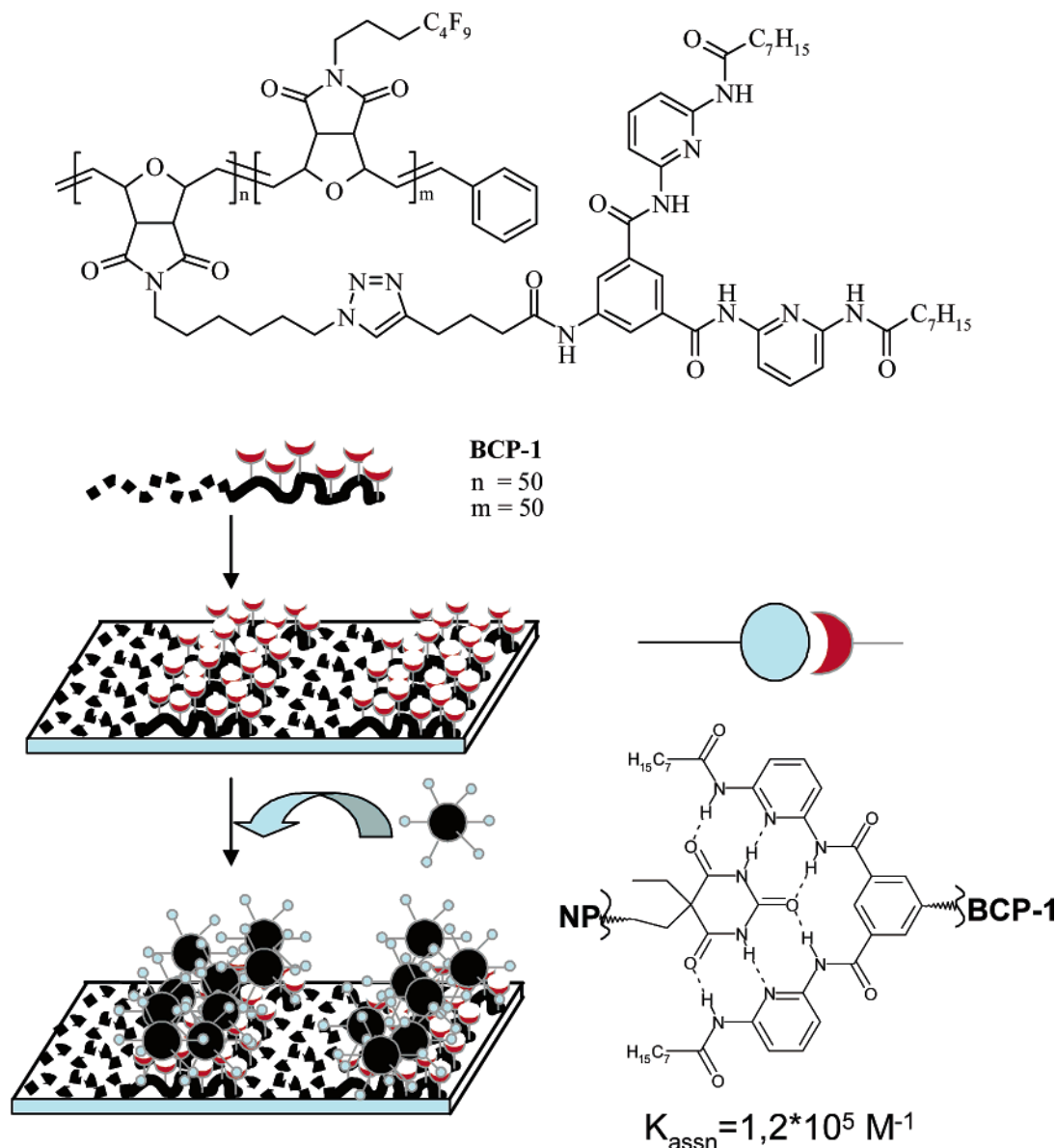


Figure 1. Strategy to bind nanoparticles (NP) onto block copolymer surfaces (BCP) via multiple hydrogen-bonding interactions (Hamilton receptor). Starting from BCP 1 a microphase-separated thin film is prepared, onto which NPs are bound subsequently.

the NanoScope software version 6.13r1 (Digital Instruments, Veeco). The roughness data used in this paper are root-mean-square (rms) values, derived as standard deviations of all height values in an image. Phase images (i.e., the phase lag between the piezo-oscillation driving the AFM cantilever and its response) have been recorded simultaneously with the topographic images through the second data channel of the instrument.

Results and Discussion. We have started our investigations with BCPs derived from poly(oxynorbornenes), where (a) the Hamilton receptor is positioned in one of the polymeric blocks and (b) a fluorinated side chain is designed into the other block to enhance the microphase separation (Figure 1). The synthesis of the BCP relied on a previously developed combination of ROMP homopolymers with “click-type” reactions,¹⁶ furnishing the corresponding BCP-1 in high yields ($M_n = 23\,800 \text{ g mol}^{-1}$, $M_n/M_w = 1.20$, $n = 50$; $m = 50$) in a short reaction sequence (Figure 2). Briefly, the two oxynorbornene monomers 4 and 5 were polymerized using the Grubbs I catalyst, furnishing the block copolymer BCP-2. After transformation into BCP-3 via

azide exchange, the Hamilton receptor 6 was attached using the azide/alkyne “click” reaction.^{16,17} Reaction yields within this synthesis were high, reaching nearly quantitative levels due to the high efficiency of the azide/alkyne “click” reaction from polymer 5 with the terminal alkyne 6. The resulting BCP-1 was cast into thin films (thickness $\sim 50 \text{ nm}$) onto silicon wafers, by either spin-casting or dip-casting. Figure 3a,b shows AFM images (topography, Figure 3a; phase image, Figure 3b) of a BCP film as derived from dip-casting (drawing speed of 3 mm/min) in THF without any further heat treatment. In the topographic image a smooth and largely homogeneous film surface with an rms roughness of 0.5 nm (0.3 nm without the holes) can be observed. Only three minor pore defects in the upper part of the image are present. The high homogeneity of the film with respect to chemical composition and surface termination is supported by the uniform appearance of the phase image. Other solvents (such as chloroform and toluene) did not yield films of sufficient quality. In fact, AFM images of films obtained with these solvents (not shown in this paper) have revealed

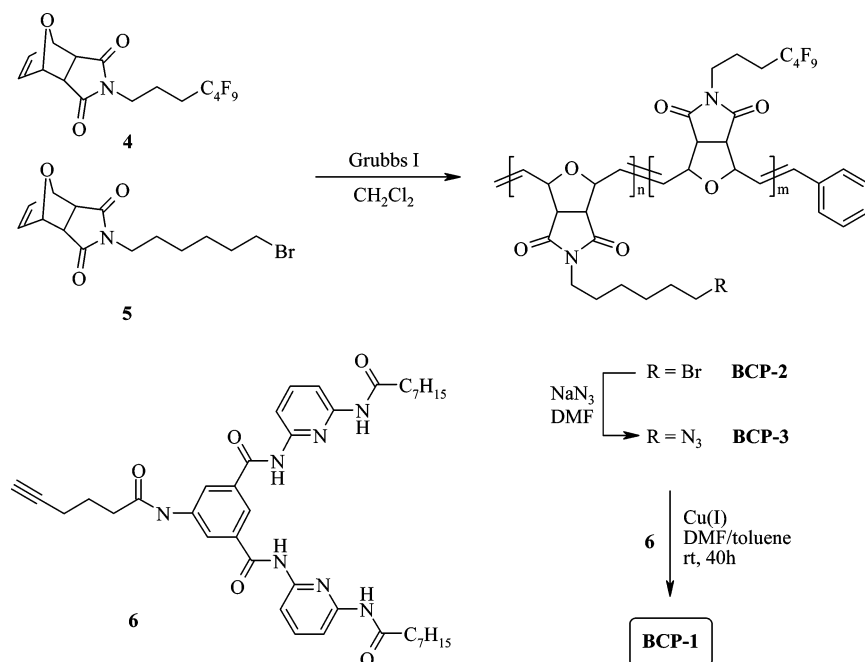


Figure 2. Preparation of BCP 1 via ROMP and subsequent azide/alkyne "click" reactions.

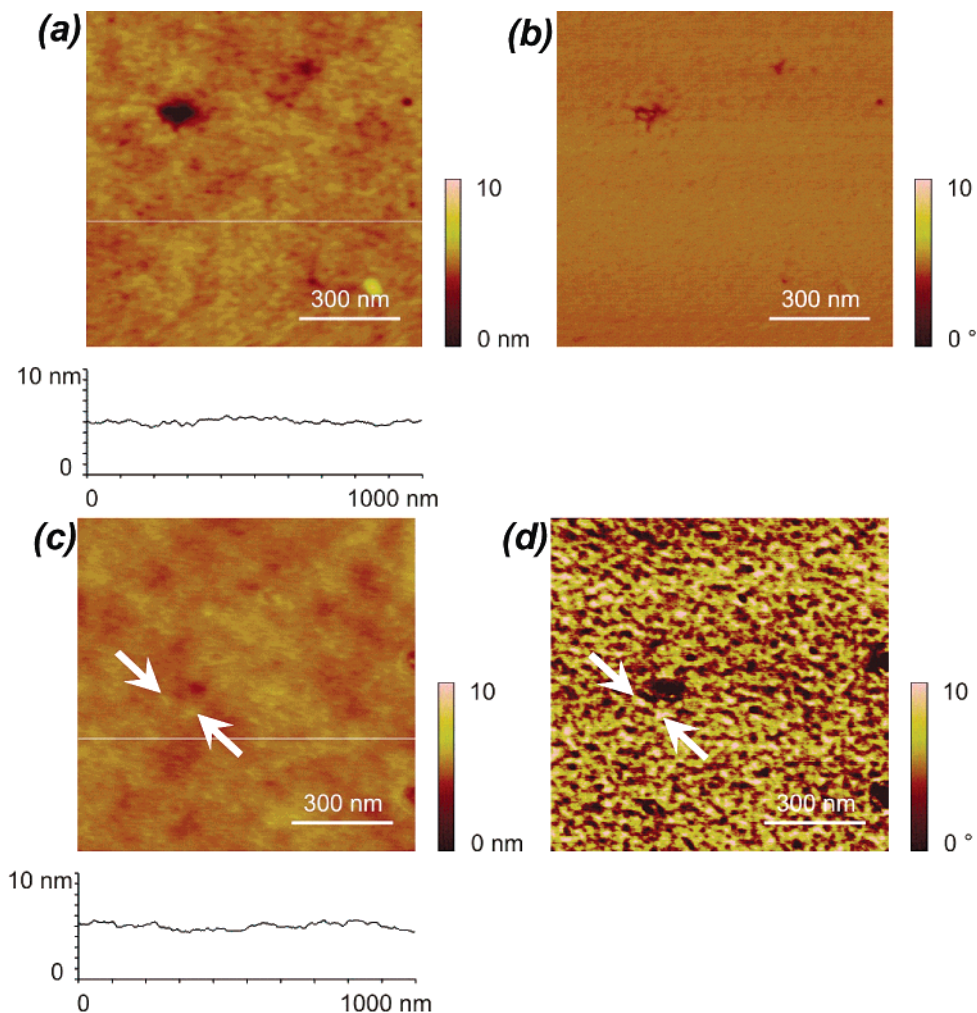


Figure 3. AFM images of thin films prepared from BCP 1 on silicon wafers. (a) Height image and (b) phase image of a directly prepared film via dip-coating from THF-solution (0.5% solution). Height (c) and phase image (d) of the same film after annealing at 80 °C for 48 h in vacuo. The bright regions in the phase image are also somewhat higher in the topographic image (see e.g. white arrows).

much more inhomogeneous films with a much higher density of pore defects than in the case of dip-casting

from THF. Annealed films (48 h, $T = 80\text{ °C}$, in vacuo) of the polymer show microphase separation in the AFM

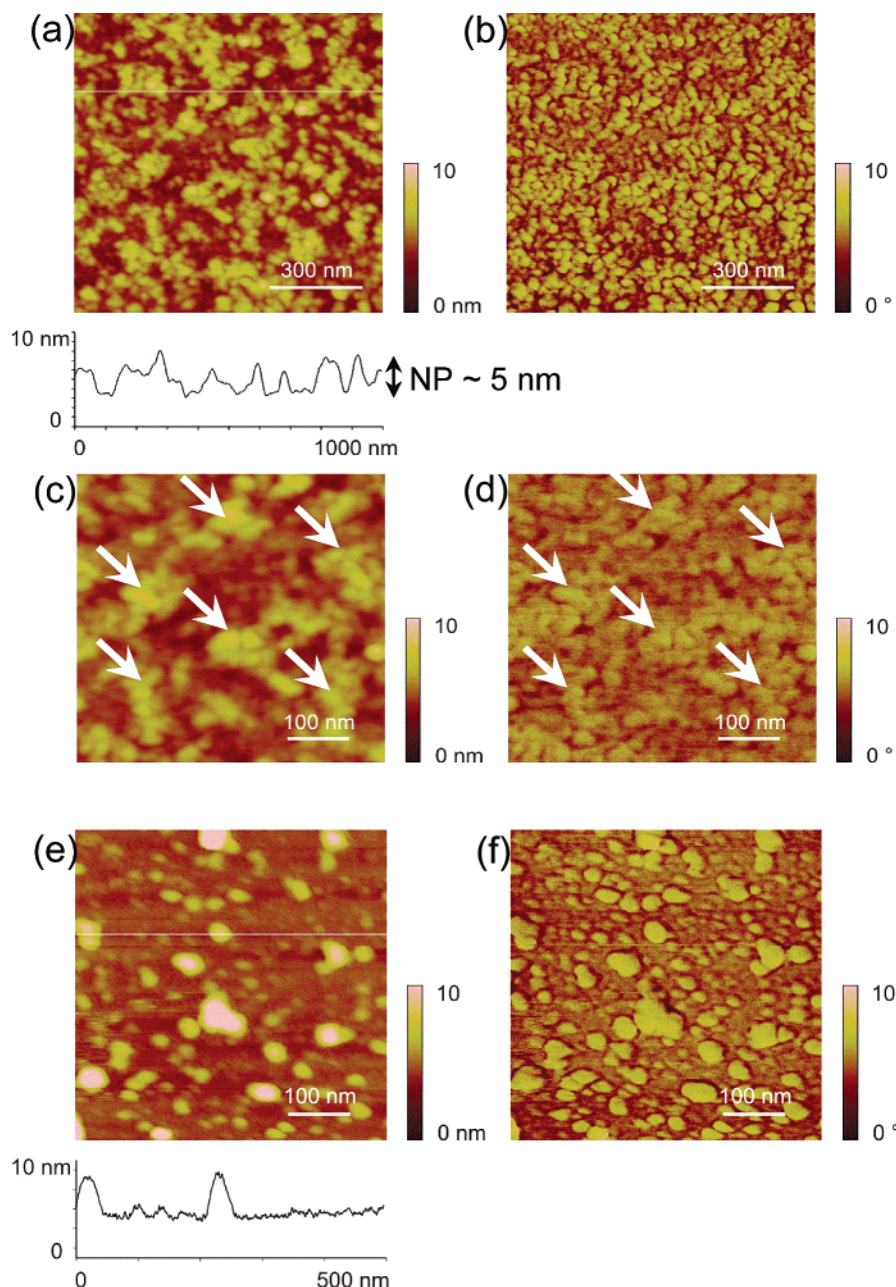


Figure 4. AFM images of polymer films after incubation with 5 nm Au-nanoparticles. (a) Height and (b) phase image of BCP-1 film incubated with NPs for 16 h. The height differences of 5 nm clearly indicate the surface-bound NPs. (c, d) Same surface recorded at higher resolution. The relevant “island-type” regions are indicated by white arrows. (e) Height and (f) phase image of a polymer film (BCP-1) after incubation with Au NPs displaying the *N,N'*-dimethylbarbituric acid receptor with a low association constant of $\sim 15 \text{ M}^{-1}$. Only some larger aggregates are visible.

phase contrast image (Figure 3d), demonstrating the formation of domains consisting of two different blocks of the BCP. Whereas the topographic image (Figure 3c) still shows a flat and homogeneous film (rms roughness = 0.3 nm), the pronounced contrast in the phase image (Figure 3d) indicates that chemical inhomogeneities through microphase separation have developed. This microphase separation leads to the formation of domains consisting of two different blocks of the BCP. From the phase image a typical diameter of these domains on the order of 15–20 nm can be derived. A closer comparison of the topographic and the phase image reveals that the bright areas in the phase image are higher (approximately 0.5–0.7 nm) in the topographic image (see e.g. arrows in Figure 3c,d). It can be assumed that the hydrophobic blocks are pointing outward from the surface, leading to slightly thicker films in these regions.

Thus, the bright areas in the phase image most likely constitute the hydrophobic portion of the phase-separated polymer film. Additionally, microphase separation in bulk BCP-1 was proven by SAXS (see Supporting Information). Since the Hamilton receptor structure is only located in one block of the BCP, it can be concluded that presentation of this receptor is effected in only one domain of the BCP on the surface. Films prepared without annealing directly from the solvent do not show microphase separation with the hydrophobic block pointing outward from the surface and the hydrophilic block being buried into the surface.

As demonstrated previously,⁵ the strength of the Hamilton receptor (surface/NP association constant = $1.2 \times 10^5 \text{ M}^{-1}$) is sufficiently high to assemble NPs (with surfaces presenting barbituric acid) with sizes of 5 and 20 nm onto SAMs presenting the Hamilton receptor.

The crucial point was the presence of multivalent interactions, thus presenting the receptor molecule in a sufficient density. Thus, it can be concluded that similar forces should act on the surface of the current phase-separated BCP-1 film, where a high density of the Hamilton receptor is present in one block (50 Hamilton receptors in the poly(oxy(norbornene) block). The binding of Au nanoparticles was effected by immersion of the BCP films into solutions containing nanoparticles functionalized with the matching barbituric acid receptor (for the preparation of the barbiturate nanoparticles see ref 5). Figure 4a shows an AFM image of the polymer film after incubation with the NPs. A pronounced topographic contrast (rms roughness = 1.1 nm) clearly indicates the attachment of the NPs. The cross-sectional profile along the white horizontal line shows a typical height for the particles of 5 nm, which is in good agreement with the nominal particle size. The lateral size of the observed features is on the order of 20–25 nm, which is in good agreement with the dimension of the phases observed in the phase image of Figure 3d. This indicates that specific binding of the particles took only place on one phase of the phase-separated polymer film. A more detailed picture of the mode of binding is revealed in Figure 4c,d, which has been recorded with higher resolution. The NPs (bright regions) bind only to specific regions (marked with white arrows in Figure c), whose size is in accordance with the domain sizes of the block copolymer. Approximately 50% of the whole area is filled with islands of NPs, whereas the other part (dark regions) is free of NPs, only presenting the other microphase of BCP-1. The presence of two different surface regions is also supported by the contrast in the phase image (Figure 4d) of the same surface area as in Figure 4c. Thus, the binding of NPs to specific parts of a microphase-separated BCP surface can be effected by use of the medium strength hydrogen bond (displaying an association constant of $K_{\text{assn}} = 1.2 \times 10^5 \text{ M}^{-1}$).

Another important point concerned the selectivity of the binding process. Thus, the BCP surface was incubated with NPs bearing *N,N*-dimethylbarbiturate moieties on their surface, which only binds to the Hamilton receptor with a relatively low association constant ($K_{\text{assn}} = 15 \text{ M}^{-1}$).⁵ The AFM images of the polymer film after incubation (16 h) with NPs functionalized with these blocked barbiturate groups are shown in Figure 4e,f. A random deposition of nanoparticulate aggregates on the surface (rms roughness = 2.5 nm), which does not reflect the phase separation pattern seen in Figure 3, can be observed. This indicates an unspecific binding of the NPs on this surface. The comparatively large sizes of the adsorbed features up to over 100 nm in diameter and over 20 nm in height indicate that agglomeration¹⁸ takes place, which in fact has already been observed in solution by dynamic light scattering measurements (data not shown).

In conclusion, we have demonstrated for the first time the selective binding of NPs onto specific regions of the microphase-separated BCP-1 by use of specific hydrogen bonds. Phase separation is achieved via a defined molecular design of the block copolymer BCP-1 and clearly seen upon generating films on silicon wafers and thermal annealing. Selective nanoparticle binding can be effected on specific regions of the BCP film, in particular those displaying the Hamilton receptor. Thus, together with the simple synthetic approach for BCP-

1, a number of related polymers can easily be prepared and used as assembly platform for appropriately surface modified NPs. Because of the large number and high specificity of hydrogen-bonding interactions, the attachment of different nanosized objects can be envisioned.

Acknowledgment. We thank the FWF for financial support (FWF 14844 CHE). Ronald Zirbs is thanked for the preparation of functionalized nanoparticles.

Supporting Information Available: Preparation of block copolymers BCP-1, BCP-2, and BCP-3; figures depicting the ¹H NMR spectra (BCP-1, BCP-2, and BCP-3), IR spectra (BCP-1, BCP-2), and DSC (BCP-1); a detailed synthetic procedure commenting on the preparation of monomer 4; TEM and DLS data of the Au nanoparticles bearing (a) a barbiturate receptor and (b) a nonbinding *N,N*-dimethylbarbiturate receptor; SAXS profiles of BCP-1 and BCP-3. This material is available free of charge via the Internet at <http://pubs.acs.org>.

References and Notes

- (a) Binder, W. H. *Angew. Chem., Int. Ed.* **2005**, 5172–5175. (b) Murray, C. B.; Kagan, C. R.; Bawendi, M. G. *Annu. Rev. Mater. Sci.* **2000**, 30, 545–610.
- (a) Maury, P.; Peter, M.; Mahalingam, V.; Reinhoudt, D. N.; Huskens, J.; *Adv. Funct. Mater.* **2005**, 15, 451–457. (b) Mahalingam, V.; Onclin, S.; Peter, M.; Ravoo, B. J.; Huskens, J.; Reinhoudt, D. N. *Langmuir* **2004**, 20, 11756–11762. (c) Crespo-Biel, O.; Dordi, B.; Reinhoudt, D. N.; Huskens, J. *J. Am. Chem. Soc.* **2005**, 127, 7594–7600.
- Auletta, T.; Dordi, B.; Mulder, A.; Sartori, A.; Onclin, S.; Bruinink, C. M.; Peter, M.; Nijhuis, C. A.; Beijleveld, H.; Schönherr, H.; Vancso, G. J.; Casnati, A.; Ungaro, R.; Ravoo, B.; Huskens, J.; Reinhoudt, D. N. *Angew. Chem., Int. Ed.* **2004**, 43, 369–373.
- Boal, A. K.; Ilhan, F.; DeRouchey, J. E.; Thurn-Albrecht, T.; Russell, T. P.; Rotello, V. M. *Nature (London)* **2000**, 404, 746–748.
- Zirbs, R.; Kienberger, F.; Hinterdorfer, P.; Binder, W. H. *Langmuir* **2005**, 21, 8414–8421.
- Baron, R.; Huang, C.-H.; Bassani, D. M.; Onopriyenko, A.; Zayats, M.; Willner, I. *Angew. Chem., Int. Ed.* **2005**, 44, 4010–4015.
- See e.g.: (a) Demers, L. M.; Ginger, D. S.; Park, J.-S.; Li, Z.; Chung, S.-W.; Mirkin, C. A. *Science* **2002**, 296, 1836–1838. (b) Chung, S.-W.; Ginger, D. S.; Morales, M. W.; Zhang, Z.; Chandrasekhar, V.; Ratner, M. A.; Mirkin, C. A. *Small* **2005**, 1, 64–69.
- See e.g.: Bhat, R. R.; Genzer, J.; Chaney, B. N.; Sugg, H. W.; Liebmann-Vinson, A. *Nanotechnology* **2003**, 14, 1145–1152 and references therein.
- See e.g.: Rogach, A. L.; Talapin, D. V.; Shevchenko, E. V.; Kornowski, A.; Hasse, M.; Weller, H. *Adv. Funct. Mater.* **2002**, 12, 653–664.
- (a) Bockstaller, M. R.; Mickiewicz, R. A.; Thomas, E. L. *Adv. Mater.* **2005**, 17, 1331–1349 and references therein. (b) For a theoretical treatment: Thompson, R. B.; Ginzburg, V. V.; Matsen, M. W.; Balazs, A. C. *Science* **2001**, 292, 2469–2472.
- (a) Minelli, C.; Geissbuehler, I.; Eckert, R.; Vogel, H.; Heinzelmann, H.; Liley, M. *Colloid Polym. Sci.* **2004**, 282, 1274–1278. (b) Minelli, C.; Hinderling, C.; Heinzelmann, H.; Pugin, R.; Liley, M. *Langmuir* **2005**, 21, 7080–7082.
- (a) Chiu, J. J.; Kim, B. J.; Kramer, E. J.; Pine, D. J. *J. Am. Chem. Soc.* **2005**, 127, 5036–5037. (b) Lin, Y.; Böker, A.; He, J.; Sill, K.; Xiang, H.; Abetz, C.; Li, X.; Wang, J.; Emrick, T.; Long, S.; Wang, Q.; Balazs, A.; Russell, T. P. *Nature (London)* **2005**, 434, 55–59. (c) Yeh, S.-W.; Wei, K.-H.; Sun, Y.; Jeng, U.-S.; Liang, K. S. *Macromolecules* **2005**, 38, 6559–6565. (d) Misner, M. J.; Skaff, H.; Emrick, T.; Russell, T. P. *Adv. Mater.* **2003**, 15, 221–224.
- (a) Boal, A. K.; Frankamp, B. L.; Uzun, O.; Tuominen, M. T.; Rotello, V. M. *Chem. Mater.* **2004**, 16, 3252–3256. (b) Shenhar, R.; Jeoung, E.; Srivastava, S.; Norsten, T. B.; Rotello, V. M. *Adv. Mater.*, in press.

- (14) (a) Sohn, B.-H.; Chio, J.-M.; Yoo, S. I.; Yun, S.-H.; Zin, W.-C.; Jung, J. C.; Kanhehara, M.; Hirata, T.; Teranishi, T. *J. Am. Chem. Soc.* **2003**, *125*, 6368–6369. (b) Yeh, S.-W.; Chang, Y.-T.; Chou, C.-H.; Wei, K.-H.; *Macromol. Rapid Commun.* **2004**, *25*, 1679–1686 and references therein.
- (15) Kwart, H.; Burchuk, I. *J. Am. Chem. Soc.* **1952**, *74*, 3094–3097.
- (16) Binder, W. H.; Kluger, C. *Macromolecules* **2004**, 9321–9330.
- (17) (a) Binder, W. H.; Kluger, C. *Curr. Org. Chem.*, in press. (b) Kolb, H. C.; Finn, M. G.; Sharpless, K. B. *Angew. Chem., Int. Ed.* **2001**, *40*, 2004–2021.
- (18) Storhoff, J. J.; Elghanian, R.; Mirkin, C. A.; Letsinger, R. L. *Langmuir* **2002**, *18*, 6666–6670.

MA0518252